UDC 541.6:546.621:546.72/.74

# ENCAPSULATION OF TRANSITION METALS IN ALUMINUM NITRIDE FULLERENE: TM@(AlN)$_{12}$ (TM = Ti, Mn, Fe, Co, AND Ni)

## C.-Y. Zhang, L.-Y. Cui, B.-Q. Wang, J. Zhang, J. Lu

*Department of Chemistry, Shanxi Normal University, Linfen, P.R. China*

The structure and stability of endohedral TM@(AlN)$_{12}$ (TM = Ti, Mn, Fe, Co, Ni ) complexes are studied at the level of density functional theory. It is found that complexes with TM = Mn, Fe, and Ni are energy minimum structures with TM at the cage center in $T_h$ symmetry, while those with TM = Ti and Co have more negative inclusion energies and the off-centered structures with TM placed towards one hexagon face in $C_1$ symmetry. The calculations predict that the HOMO and LUMO energy gap of TM@(AlN)$_{12}$ differs from those of the (AlN)$_{12}$ cage and a free TM atom. The amount of charge that is transferred from the encapsulated guests to the cage increases with the atomic radius. The electronic and magnetic properties of TM@(AlN)$_{12}$ are discussed.

**K e y w o r d s:** density functional theory, endohedral complexes, inclusion energy, energy gap, deformation energy.

### INTRODUCTION

Aluminum nitride (AlN) ceramics have attracted research interests so far because of their excellent physical and chemical properties (high thermal conductivity, low thermal-inflate coefficient, chemical inertness, and large HOMO-LUMO energy gap) [1—8]. After the exhaustive exploration of the electronic properties of silicon, the need for new materials with different properties has drawn much attention to nanoscale aluminum nitride semiconductor structures [9—13]. Metal-containing endohedral fullerenes have attracted special attention as a new class of technologically relevant materials due to their combined fullerene-like and metallic properties. Up to now, many metallofullerenes have been synthesized [14]. Although some AlN clusters are studied theoretically and experimentally [15—28], there are no reports on the study of TM@(AlN)$_n$, where TM is a transition metal atom included in (AlN)$_n$ cages. The TM atom, such as Ti, Mn, Fe, Co, and Ni, is especially intriguing due to the nature of metal—metal bonds involving the metal *s*, *p*, and *d* orbitals. The $T_h$ symmetrical (AlN)$_{12}$ cluster is the most stable among (AlN)$_n$ cages [26]. When the TM atom is encapsulated into the (AlN)$_{12}$ cage, the cluster may exhibit novel electronic, magnetic, and chemical behavior. In this paper, we report the structures, stabilities, and electronic properties of endohedral TM@(AlN)$_{12}$ complexes (TM = Ti, Mn, Fe, Co, and Ni ) at the level of spin-polarized density functional theory (DFT). The present study gives us a guideline for the design and synthesis of these new metallofullerene clusters that are very promising as nanoscale devices.

### COMPUTATIONAL METHODS

All the calculations were performed at the spin-polarized DFT level with the Perdew and Wang functional (GGA-PW91) [29] using the DMol3 program [30—32] in the Materials Studio of Accelrys Inc. The double numerical basis set augmented with *d*-polarization was utilized, and ionic cores of

*The natural charges ($q_{TM}$), bond distances ($R$, Å), total spin density ($S$) and the radium of metal atom ($r_{TM}$, Å) of $(AlN)_{12}$ and $TM@(AlN)_{12}$ clusters*

| Cluster | $r_{TM}$ [a] | $q_N$ | $q_{Al}$ | $q_{TM}$ | $R_{N—Al}$ [b] | $R_{N—Al}$ [c] | $R_{TM—Al}$ | $R_{TM—N}$ | $S$ |
|---|---|---|---|---|---|---|---|---|---|
| $(AlN)_{12}$ ($T_h$) | — | −1.830 | 1.830 | — | 1.800 | 1.865 | (2.767) | (3.004) | — |
| $Ti@(AlN)_{12}$ ($C_1$) | 1.320 | −1.801 [d] | 1.715 [d] | 1.030 | 1.838 [e] | 1.897 [e] | 2.592 [f] | 2.021 [f] | 0.01 |
| $Mn@(AlN)_{12}$ ($T_h$) | 1.170 | −1.840 | 1.787 | 0.638 | 1.818 | 1.870 | 2.842 | 3.004 | 4.78 |
| $Fe@(AlN)_{12}$ ($T_h$) | 1.165 | −1.817 | 1.783 | 0.418 | 1.815 | 1.870 | 2.784 | 3.028 | 3.91 |
| $Co@(AlN)_{12}$ ($C_1$) | 1.160 | −1.820 [d] | 1.784 [d] | 0.411 | 1.814 [e] | 1.877 [e] | 2.539 [f] | 2.631 [f] | 2.81 |
| $Ni@(AlN)_{12}$ ($T_h$) | 1.150 | −1.813 | 1.780 | 0.396 | 1.812 | 1.870 | 2.768 | 3.032 | 1.76 |

[a] N.N. Greenwood, A. Earnshaw, Chemistry of the Elements, second ed., Elsevier, 1997.

[b] The N—Al bond fusing two 6-ring.

[c] The N—Al bond between a 4- and a 6-ring.

[d] Average value obtained by summing the natural charge for all atoms (either N or Al) and dividing by the total number of atoms.

[e] Average value obtained by summing the bond distances for all N—Al (either on 6/6 or on 4/6) and dividing by the total number of bonds.

[f] The TM—Al(N) average bond distances to the adjacent cage face.

The numbers in parentheses represent the distance from the cage center to a vertex, N or Al.

the metal were described by the effective core potential (ECP). For the numerical integration, a fine quality mesh size was used, and the real space cutoff of the atomic orbital was set at 5.5 Å. The convergence criteria for structure optimization and energy calculations were set to FINE with the tolerance for density convergence in SCF, energy, gradient, and displacement of $1 \times 10^{-6}$ $e$/Å, $2 \times 10^{-5}$ a.u., $4 \times 10^{-4}$ Å, and $5 \times 10^{-4}$ Å respectively. All reported complexes have been characterized as energy minimum structures by the corresponding frequency calculations (the number of imaginary frequencies is zero, $N_{imag} = 0$). The energies and physical properties for discussion have also been computed by the same way. In addition, the atomic charges were evaluated using natural bond orbital (NBO) analysis [33]. The results are presented in Tables 1, 2 and optimized structures are shown in Figs. 1 and 2.

*Total electronic energies ($E_{tot}$, a.u.), the first vibrational frequency ($\nu_1$, cm$^{-1}$), number of imaginary frequencies ($N_{imag}$), zero-point energies (ZPE, kcal/mol), LOMO-HOMO gap ($\Delta E_g$, eV), inclusion energies ($\Delta E_{inc}$, kcal/mol) and deformation energies ($\Delta E_{def}$, kcal/mol) of complex structures*

| Cluster | $E_{tot}(N_{imag})$ | $\nu_1$ | ZPE | $\Delta E_g$ [a] | $\Delta E_{inc}$ [b] | $\Delta E_{def}$ [c] |
|---|---|---|---|---|---|---|
| $(AlN)_{12}$ | −3567.3135(0) | 152.3 | 47.87 | 2.66 | — | 0.00 |
| $Ti@(AlN)_{12}$ | −3625.7050(0) | 51.5 | 45.49 | 0.52(0.23) | −73.29 | 119.35 |
| $Mn@(AlN)_{12}$ | −3671.6919(0) | 65.1 | 44.64 | 0.39(1.94) | −66.20 | 10.54 |
| $Fe@(AlN)_{12}$ | −3691.2442(0) | 50.7 | 45.93 | 0.89(0.16) | −52.21 | 3.51 |
| $Co@(AlN)_{12}$ | −3713.2667(0) | 41.4 | 46.08 | 0.88(0.04) | −66.64 | 6.96 |
| $Ni@(AlN)_{12}$ | −3738.4062(0) | 49.6 | 46.21 | 1.12(2.99) | −45.75 | 2.82 |

[a] The values of free TM atom are in parenthesis.

[b] Inclusion energy: $\Delta E_{inc} = E(TM@(AlN)_{12} - [E(TM) + E(AlN)_{12}]$.

[c] $\Delta E_{def} = E(AlN)_{12}(strain) - E(AlN)_{12}$ is the deformation energy of cage $(AlN)_{12}$ due to TM insertion.
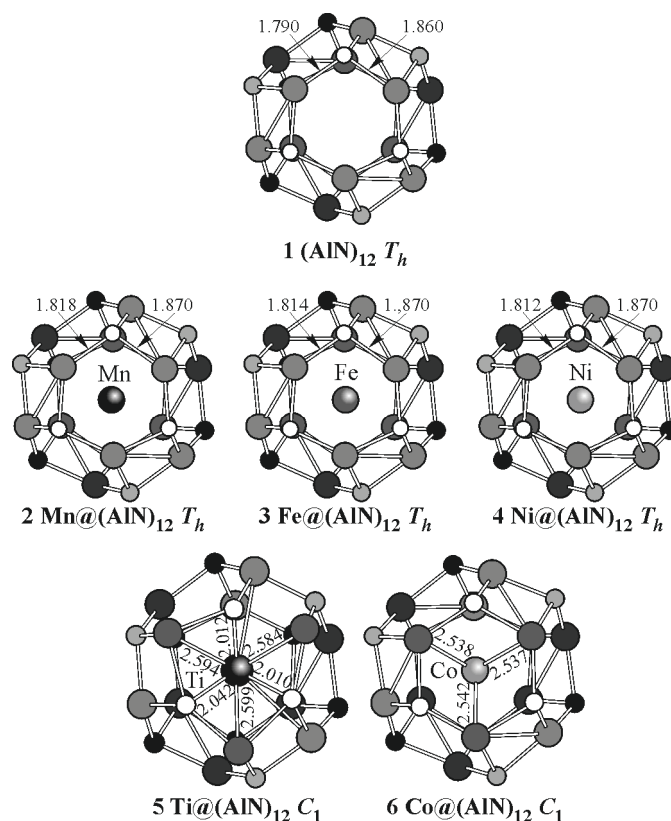
*Fig. 1.* $(AlN)_{12}$ and various endohedral $TM@(AlN)_{12}$ structures

## RESULTS AND DISCUSSION

**1. Structures and charge distribution.** As found previously [34, 35], the most stable $(AlN)_{12}$ cage has the $T_h$ symmetry with six four-membered rings and eight six-membered rings. This structure obeys exactly the isolated square rule [36], namely, the six-four-membered rings have the maximum separation. To determine the ground state geometry of $TM@(AlN)_{12}$ (TM = Ti, Mn, Fe, Co, and Ni), we tried different initial configurations with $T_h$ symmetry and other endohedral structures of lower symmetry, in which the TM atom is placed close to the cage center or to one of the hexagon faces. The optimized structures and geometrical parameters of the complexes are shown in Fig. 1 and Table 1. Among them, the $TM@(AlN)_{12}$ (TM = Mn, Fe, and Ni) complexes are still stable and keep the $T_h$ symmetry, whereas the local minima for $Ti@(AlN)_{12}$ and $Co@(AlN)_{12}$ have the $C_1$ symmetry, and both Ti and Co are located near one of the hexagon faces. Herein, let us first analyze the structural changes caused by the insertion of TM into the $(AlN)_{12}$ cage.

For the $T_h$ symmetrical series (TM = Mn, Fe, and Ni) the cage-centered Mn, Fe, and Ni endohedral complexes are the local minima, as Fig. 1 displays. From Table 1, when guest TM is introduced into the cage, we can see that the cage skeleton swells slightly and tends to be a sphere, and the 4- and 6-membered rings both deviate from the plane. In detail, as compared to the empty cage, the skeletal N—Al bond lengths on 6/6 and 4/6 also increase in turn, but the change extent of the N—Al bond lengths on the 6/6 ring is small (1.818 Å, 1.815 Å, and 1.812 Å respectively) with the increase in TM radii, while those on the 4/6 ring generally do not have any change (1.870 Å). In addition, the distances between the cage center and the apex N and Al atoms all increase (Table 1), but the changes are small (< 0.07 Å).

The amount of charge transfer that occurs within each TM complex was quantified according to the NBO analysis. Aluminum is an electron-deficient atom; N has relatively stronger electronegativity. So, the $(AlN)_{12}$ compound has an obvious electron accepting ability. When a guest TM atom is introduced into the cage, the partial electron transfer occurs from the TM atom onto the cage (0.64 *e* from
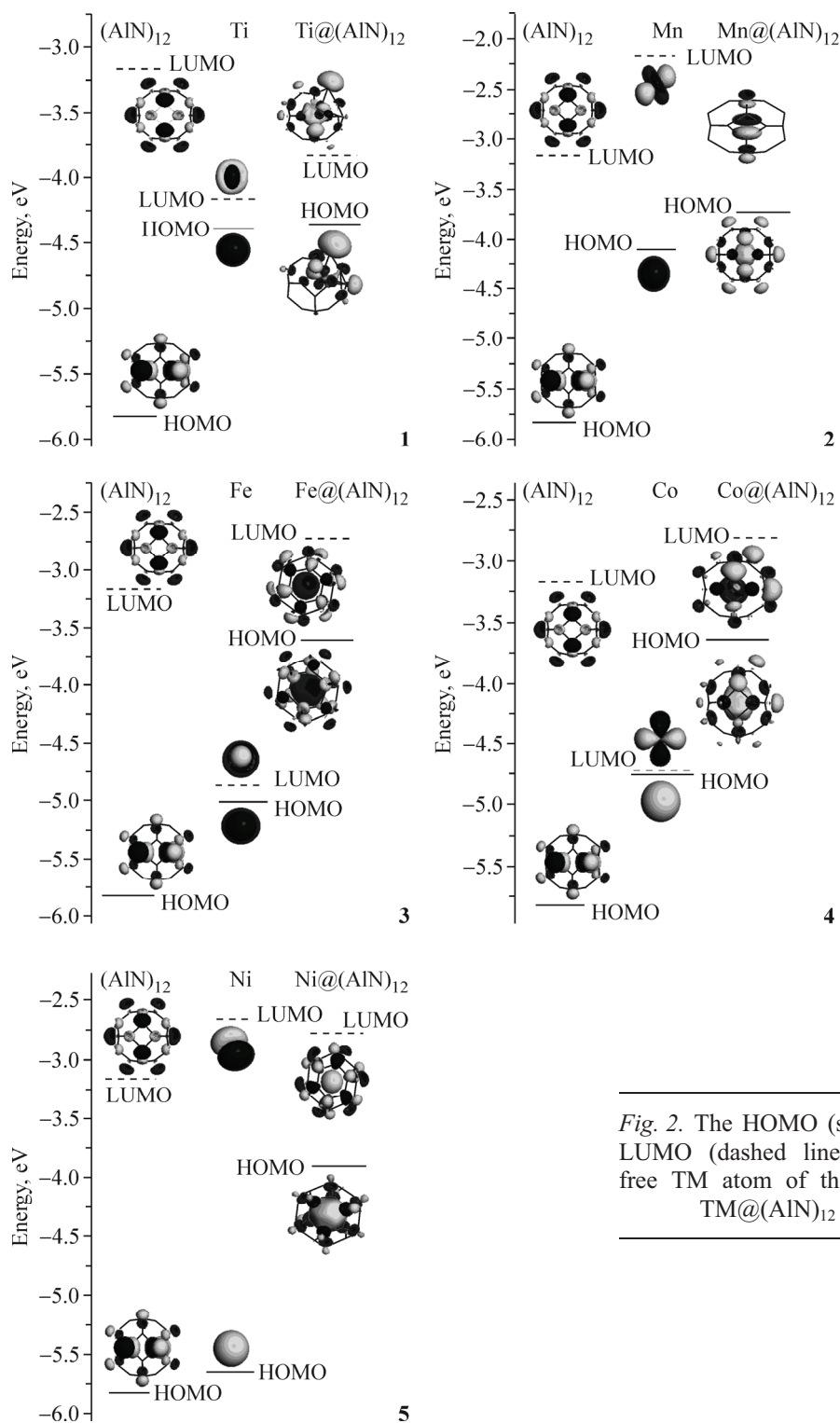
*Fig. 2.* The HOMO (solid line) and LUMO (dashed line) of $(AlN)_{12}$, free TM atom of the most stable TM@$(AlN)_{12}$ cages

Mn, 0.42 $e$ from Fe, and 0.40 $e$ from Ni). It appears that the amount of charge transfer increases with an increase in the atom radius (Table 1). The results confirm that the $(AlN)_{12}$ cage has the property of storing electrons.

For the Ti@$(AlN)_{12}$ complexes of the $C_1$ symmetry, the Ti guest is shifted significantly (by 0.984 Å) from the cage center; the average Ti—Al and Ti—N bond lengths are 2.592 Å and 2.021 Å which indicates noticeable bonding interactions between Ti and Al and N atoms. Meanwhile, the Al—N average

distances on 6/6 and 4/6 rings are elongated from 1.800 Å and 1.865 Å in the parent cage to 1.838 Å and 1.897 Å in Ti@(AlN)$_{12}$.

Akin to the Ti atom, the Co guest is also off-centered by 0.40 Å and locates near one of the six-membered rings and has a distance of 1.793 Å to the center of this ring, where Co is only bound to the adjacent Al atom and has the average bond length of 2.539 Å, whereas the distance (2.631 Å) between Co and its adjacent N atom is too large to form Co—N bonds. As expected, the Al—N average distances on 6/6 and 4/6 rings are elongated, and the average values are more than those of the parent cage by 0.014 Å and 0.012 Å.

In addition, when Ti and Co atoms are introduced into the cage, partial electron transfer occurs from the guests to the cage (as shown in Table 1). As a result, TM atoms have positive charges (1.030 on Ti and 0.411 on Co).

**2. Energy parameters and stability.** In addition to the structures, we have also computed the inclusion energies ($\Delta E_{inc}$), thermodynamic values ($\Delta Z$), and deformation energies ($\Delta E_{def}$) for the encapsulation of a TM atom. The values of $\Delta E_{inc}$ and $\Delta Z$ of the endohedral complexes are estimated as the difference in the energy parameters of TM@(AlN)$_{12}$ and the isolated components ((AlN)$_{12}$ and the TM atom). Actually, $\Delta E_{inc}$ and $\Delta Z$ indicate the sum of electrostatic and bonding interactions between the encapsulated TM atom and the (AlN)$_{12}$ cage. As shown in Table 2, $\Delta E_{inc}$ and $\Delta Z$ of the endohedral complexes are negative, showing that the formation of TM@(AlN)$_{12}$ is exothermic and energetically favorable.

The deformation energy is the energy change in the parent cage due to TM insertion. As expected, the values are in line with the increase in the TM atomic radii (Table 2).

For the $T_h$ symmetrical series, $\Delta E_{inc}$ generally become more negative along with the increase in the atomic radii; the $\Delta E_{inc}$ values for Mn, Fe, and Ni are –66.2 kcal/mol, –52.2 kcal/mol, and –45.8 kcal/mol respectively. For the Mn guest with the maximum caged radius, the value of $\Delta E_{inc}$ is the most negative. Thus, Mn@(AlN)$_{12}$ is the most stable endohedral structure of the examined series. In comparison, other $T_h$ symmetrical complexes have moderate thermodynamic stabilities.

In addition, $\Delta E_{def}$ correlate with the TM atomic radii. For the $T_h$ symmetry series, the larger the guest TM radius, the larger the deformation energy and the lower the stability of the endohedral structure, but it constitutes only a small fraction of the energy released when an internal TM guest is expelled from a cage.

As shown in Table 2, $\Delta E_{inc}$ and $\Delta E_{def}$ for the $C_1$ symmetrical clusters are larger than those of the $T_h$ structures. This can be rationalized in terms of orbital interactions between TM and the AlN fullerene cage. The larger effect of Ti and Co can be explained by significant bonding interactions of these atoms with the atoms of the neighboring ring (Fig. 1). $\Delta E_{inc}$ is a key factor in the estimation of the complex stability. Consequently, the thermodynamic stability of TM@(AlN)$_{12}$ structures could be ranged as follows: Ti@(AlN)$_{12}$ > Co@(AlN)$_{12}$ > Mn@(AlN)$_{12}$ > Fe@(AlN)$_{12}$ > Ni@(AlN)$_{12}$.

### CONCLUSIONS

DFT calculations have been carried out on the structure and stability as well as the electronic properties of the endohedral TM@(AlN)$_{12}$ (TM = Ti, Mn, Fe, Co, and Ni) complexes. The most stable TM@(AlN)$_{12}$ (TM = Ti, Mn, Fe, Co, and Ni) complexes have $C_1$, $T_h$, $T_h$, $C_1$, and $T_h$ symmetries respectively, and they are energetically favorable. For the $T_h$ symmetrical series (TM = Mn, Fe, and Ni) and $C_1$ symmetrical series (TM = Ti and Co), their inclusion energies and thermodynamic values of the endohedral complexes are negative, and therefore, the complexes are thermodynamically stable. In addition, their energy parameters are respectively enhanced along with the increased TM atomic radii. The doped TM atoms are positively charged due to charge transfer; there are strong electrostatic and orbital interactions between the guest and the host. With the exception of Ti@(AlN)$_{12}$, the other endohedral structures have nearly the same spin density as free TM atoms.

## REFERENCES

1. *Ponce F.A., Bour D.P.* // Nature (London). – 1997. – **386**. – P. 351.
2. *Kiehne G.T., Wong G.K.L., Ketterson J.B.* // J. Appl. Phys. – 1998. – **84**. – P. 5922.
3. *Krupitskaya R.Y., Auner G.W.* // J. Appl. Phys. – 1998. – **84**. – P. 2861.
4. *Kuo P.K., Auner G.W., Wu Z.L.* // Thin Solid Films. – 1994. – **253**. – P. 223.
5. *Ruiz E., Alvarez S., Alemany P.* // Phys. Rev. B. – 1994. – **49**. – P. 7115.
6. *Wang X.D., Jiang W., Norton M.G., Hipps K.W.* // Thin Solid Films. – 1994. – **251**. – P. 121.
7. *Kotula P.G., Carter C.B., Norton M.G.* // J. Mater. Sci. Lett. – 1994. – **13**. – P. 1275.
8. *Rille E., Zarwasch R., Pulker H.K.* // Thin Solid Films. – 1993. – **228**. – P. 215.
9. *Sun Q., Wang Q., Gong X.G., Kumar V., Kawazoe Y.* // Eur. Phys. J. D. – 2002. – **18**. – P. 77.
10. *Kandalam K., Pandey R., Blanco M.A., Costales A., Recio J.M., Newsam J.M.* // J. Phys. Chem. B. – 2000. – **104**. – P. 4361.
11. *Jackson T.B., Virkar A.V., More K.L., Dinwiddie R.B., Cutler R.A.* // J. Amer. Ceram. Soc. – 1997. – **80**. – P. 1421.
12. *Moura F.J., Munz R.J.* // J. Amer. Ceram. Soc. – 1997. – **80**. – P. 2425.
13. *Bradshaw S.M., Spicer J.L.* // J. Amer. Ceram. Soc. – 1999. – **82**. – P. 2293.
14. *Shinohara H.* // Rep. Prog. Phys. – 2000. – **63**. – P. 843.
15. *BelBruno J.J.* // Chem. Phys. Lett. – 1999. – **313**. – P. 795.
16. *Boo B.H., Liu Z.* // J. Phys. Chem. A. – 1999. – **103**. – P. 1250.
17. *BelBruno J.J.* // Heteroat. Chem. – 2000. – **11**. – P. 281.
18. *Wu H., Zhang C., Xu X., Zheng L., Zhang Q.* // Sci. China., Ser. B: Chem. – 2000. – **43**. – P. 634.
19. *Andrews L., Zhou M., Chertihin G.V., Bare W.J., Hannachi Y.* // J. Phys. Chem. A. – 2000. – **104**. – P. 1656.
20. *Kandalam K., Pandey R., Blanco M.A., Costales A., Recio J.M., Newsam J.M.* // J. Phys. Chem. B. – 2000. – **104**. – P. 4361.
21. *Kandalam K., Blanco M.A., Pandey R.* // J. Phys. Chem. B. – 2001. – **105**. – P. 6080.
22. *Chang C., Patzer A.B.C., Sedlmayr E., Steinke T., Sulzle D.* // Chem. Phys. Lett. – 2001. – **271**. – P. 283.
23. *Leskiw D., Castleman A.W. Jr., Ashman C., Khanna S.N.* // J. Chem. Phys. – 2001. – **114**. – P. 1165.
24. *Kandalam K., Blanco M.A., Pandey R.* // J. Phys. Chem. B. – 2002. – **106**. – P. 1945.
25. *Costales A., Blanco M.A., Martın Pendas A., Kandalam A.K., Pandey R.* // J. Amer. Chem. Soc. – 2002. – **124**. – P. 4116.
26. *Wu H., Zhang F., Xu Z., Zhang X., Jiao H.* // J. Phys. Chem. A. – 2003. – **107**. – P. 204.
27. *Li Y., Brenner D.W.* // Phys. Rev. Lett. – 2004. – **92**. – P. 075503.
28. *Meloni G., Gingerich K.A.* // J. Phys. Chem. – 2000. – **113**. – P. 10978.
29. *Perdew J.P., Wang Y.* // Phys. Rev. B. – 1992. – **45**. – P. 13244.
30. *Delley B.* // J. Chem. Phys. – 1990. – **92**. – P. 508.
31. *Delley B.* // J. Phys. Chem. – 1996. – **100**. – P. 6107.
32. *Delley B.* // J. Chem. Phys. – 2000. – **113**. – P. 7756.
33. *Reed E., Curtiss L.A., Weinhold F.* // Chem. Rev. – 1988. – **88**. – P. 899.
34. *Sun M.L., Slanina Z., Lee S.L.* // Chem. Phys. Lett. – 1995. – **233**. – P. 279.
35. *Slanina Z., Sun M.L., Lee S.L.* // Nanostructured Mater. – 1997. – **8**. – P. 623.
36. *Fowler P.W., Heine T., Mitchell D., Schmidt R., Seifert G.* // J. Chem.Soc, Faraday Trans. – 1996. – **92**. – P. 2197.
37. *Kessler B., Bringer A., Cramm S., Schlebusch C., Eberhardt W., Suzuki S., Achiba Y., Esch F., Barnaba M., Cocco D.* // Phys. Rev. Lett. – 1997. – **79**. – P. 2289.
38. *Lu J., Zhang X., Zhao X.* // Chem. Phys. Lett. – 2000. – **332**. – P. 51.
39. *Lu J., Zhang X., Zhao X.* // Chem. Phys. Lett. – 2000. – **332**. – P. 219.
40. *Lu J., Zhou Y., Zhang X., Zhao X.* // Chem. Phys. Lett. – 2002. – **352**. – P. 8.